

All-optical modulation using two-photon absorption in silicon core optical fibers

P. Mehta,¹ N. Healy,¹ T. D. Day,² J. R. Sparks,² P. J. A. Sazio,¹
J. V. Badding,² and A. C. Peacock^{1,*}

¹*Optoelectronics Research Centre, University of Southampton, Southampton SO17 1BJ, UK*

²*Department of Chemistry and Materials Research Institute, Pennsylvania State University,
Pennsylvania 16802, USA*

[*acp@orc.soton.ac.uk](mailto:acp@orc.soton.ac.uk)

Abstract: All-optical modulation based on degenerate and non-degenerate two-photon absorption (TPA) is demonstrated within a hydrogenated amorphous silicon core optical fiber. The nonlinear absorption strength is determined by comparing the results of pump-probe experiments with numerical simulations of the coupled propagation equations. Subpicosecond modulation is achieved with an extinction ratio of more than 4dB at telecommunications wavelengths, indicating the potential for these fibers to find use in high speed signal processing applications.

© 2011 Optical Society of America

OCIS codes: (060.2290) Fiber materials; (160.6000) Semiconductor materials; (190.4370) Nonlinear optics, fibers.

References and links

1. K. Narayanan and S. F. Preble, "Optical nonlinearities in hydrogenated amorphous silicon waveguides," *Opt. Express* **18**, 8998–9005 (2010).
2. Y. Shoji, T. Ogasawara, T. Kamei, Y. Sakakibara, S. Suda, K. Kintaka, H. Kawashima, M. Okano, T. Hasama, H. Ishikawa, and M. Mori, "Ultrafast nonlinear effects in hydrogenated amorphous silicon wire waveguide," *Opt. Express* **18**, 5668–5673 (2010).
3. K. Narayanan, A. W. Elshaari, and S. F. Preble, "Broadband all-optical modulation in hydrogenated-amorphous silicon waveguides," *Opt. Express* **18**, 9809–9814 (2010).
4. S. Clemmen, A. Perret, S. K. Selvaraja, W. Bogaerts, D. van Thourhout, R. Baets, P. Emplit, and S. Massar, "Generation of correlated photons in hydrogenated amorphous-silicon waveguides," *Opt. Lett.* **35**, 3483–3485 (2010).
5. B. Kuyken, S. Clemmen, S. K. Selvaraja, W. Bogaerts, D. van Thourhout, P. Emplit, S. Massar, G. Roelkens, and R. Baets, "On-chip parametric amplification with 26.5 dB gain at telecommunications wavelengths using CMOS-compatible hydrogenated amorphous silicon waveguides," *Opt. Lett.* **36**, 552–554 (2011).
6. L. Lagonigro, N. Healy, J. R. Sparks, N. F. Baril, P. J. A. Sazio, J. V. Badding, and A. C. Peacock, "Low loss silicon fibers for photonics applications," *Appl. Phys. Lett.* **96**, 041105 (2010).
7. J. Ballato, T. Hawkins, P. Foy, R. Stolen, B. Kokuoz, M. Ellison, C. McMillen, J. Reppert, A. M. Rao, M. Daw, S. Sharma, R. Shori, O. Stafsudd, R. R. Rice, and D. R. Powers, "Silicon optical fiber," *Opt. Express* **16**, 18675–18683 (2008).
8. N. Healy, J. R. Sparks, M. N. Petrovich, P. J. A. Sazio, J. V. Badding, and A. C. Peacock, "Large mode area silicon microstructured fiber with robust dual mode guidance," *Opt. Express* **17**, 18076–18082 (2009).
9. N. Healy, J. R. Sparks, R. He, P. J. A. Sazio, J. V. Badding, and A. C. Peacock, "High index contrast semiconductor ARROW and hybrid ARROW fibers," *Opt. Express* **19**, 10979–10985 (2011).
10. D. J. Won, M. O. Ramirez, H. Kang, V. Gopalan, N. F. Baril, J. Calkins, J. V. Badding, and P. J. A. Sazio, "All-optical modulation of laser light in amorphous silicon-filled microstructured optical fibers," *Appl. Phys. Lett.* **91**, 161112 (2007).
11. T. Liang, L. Nunes, T. Sakamoto, K. Sasagawa, T. Kawanishi, M. Tsuchiya, G. Priem, D. Van Thourhout, P. Dumon, R. Baets, and H. Tsang, "Ultrafast all-optical switching by cross-absorption modulation in silicon wire waveguides," *Opt. Express* **13**, 7298–7303 (2005).

12. P. Mehta, N. Healy, N. F. Baril, P. J. A. Sazio, J. V. Badding, and A. C. Peacock, "Nonlinear transmission properties of hydrogenated amorphous silicon core optical fibers," *Opt. Express* **18**, 16826–16831 (2010).
13. J. Y. Lee, L. H. Yin, G. P. Agrawal, and P. M. Fauchet, "Ultrafast optical switching based on nonlinear polarization rotation in silicon waveguides," *Opt. Express* **18**, 11514–11523 (2010).
14. R. Dekker, A. Driessen, T. Wahlbrink, C. Moormann, J. Niehusmann, and M. Först, "Ultrafast Kerr-induced all-optical wavelength conversion in silicon waveguides using 1.55 μm femtosecond pulses," *Opt. Express* **14**, 8336–8346 (2006).
15. P. Mehta, N. Healy, R. Slavík, R. T. Watts, J. R. Sparks, T. D. Day, P. J. A. Sazio, J. V. Badding, and A. C. Peacock, "Nonlinearities in silicon optical fibers," in *Optical Fiber Communication Conference*, OSA Technical Digest (CD) (Optical Society of America, 2011), paper OThS3.
16. N. Minamikawa and K. Tanaka, "Nonlinear optical properties of hydrogenated amorphous Si films probed by a novel z-scan technique," *Jpn J. Appl. Phys.* **45**, L960–L962 (2006).
17. M. Sheik-Bahae, J. Wang, and E. W. Van Stryland, "Non-degenerate optical Kerr effect in semiconductors," *IEEE J. Quantum Electron.* **30**, 249–255 (1994).

1. Introduction

Hydrogenated amorphous silicon (a-Si:H) is emerging as an increasingly promising material for photonics applications as it offers simple and flexible fabrication and possesses a large optical nonlinearity [1]. To date, a number of important photonic functions have been demonstrated in a-Si:H waveguides on-chip including all-optical modulation [2, 3], photon pair generation [4], and parametric amplification [5]. The ability to incorporate silicon materials into the optical fiber geometry not only provides a route towards integrating such devices within existing fiber networks [6, 7], but also opens up the potential for the waveguiding properties of the devices to be manipulated in ways not possible on-chip [8, 9]. As such, a-Si:H core fibers can be expected to offer new capabilities in future generations of semiconductor photonic devices.

Previous investigations in amorphous silicon core fibers have shown that it is possible to optically modulate light guided in the core at MHz frequencies via the plasma dispersion effect [10]. Unfortunately such carrier-injection modulation schemes, whether excited optically or via an external current, are limited in response speed and the free-carrier lifetime which typically ranges from hundreds of picoseconds in nanoscale silicon wires, to hundreds of nanoseconds in micron-sized waveguides. However, cross-absorption modulation (XAM) schemes based on two photon absorption (TPA) have been demonstrated which allow for high speed operation [11]. In this process, a high intensity pump pulse is co-propagated with a weak probe through the silicon waveguide. Provided that the sum of the photon energies is greater than the bandgap energy of silicon, one photon from the pump and another from the probe can be absorbed by means of phonon assisted TPA. As a result, photons are removed from the probe so that the modulation is an inversion of the pump pulse.

In this paper, we investigate XAM in a low loss a-Si:H core fiber to demonstrate its use for ultrafast all-optical modulation. The void-free semiconductor core fiber was fabricated using a high pressure microfluidic chemical deposition technique in which a mixture of silane and helium (SiH_4/He) was configured to flow down a silica capillary whilst being heated in a furnace [6]. By keeping the deposition temperatures below 450°C, the dissociation of hydrogen from the precursor is not complete so that some remains in the core to passivate the dangling bonds, greatly reducing the optical transmission loss. It is important to note that the a-Si:H fiber core material deposited using this method differs from that of the on-chip waveguides fabricated via plasma enhanced chemical vapor deposition in terms of the hydrogen content, and thus can be expected to exhibit different nonlinear parameters [1, 12]. A series of pump-probe measurements were undertaken to determine the degenerate and non-degenerate TPA parameters and to characterize the response time of the nonlinear absorption. The values obtained by fitting the results with simulations based on a set of coupled propagation equations are in good agreement with previous reports for a-Si:H waveguides on-chip. To complete our experiments,

we demonstrate the modulation of a continuous wave (CW) probe using non-degenerate TPA and discuss the effects of free-carrier absorption (FCA) on the overall device performance.

2. Theory

Since we are primarily concerned with the temporal characteristics induced on the probe via the XAM process, it is convenient to use a simplified pulse propagation model that accounts for the rate of change in the carrier density but neglects the effects of spectral modulation. Under these conditions, the coupled equations for the input fields and the carrier density are [13]:

$$\frac{\partial A_2(t, z)}{\partial z} = -\frac{\alpha_{l,2}}{2} A_2(t, z) - \frac{1}{2} \sigma_{\text{FCA}} N(t, z) A_2(t, z) - \beta'_{\text{TPA}} I_1(t, z) A_2(t, z), \quad (1a)$$

$$\frac{\partial I_1(t, z)}{\partial z} = -\alpha_{l,1} I_1(t, z) - \sigma_{\text{FCA}} N(t, z) I_1(t, z) - \beta_{\text{TPA}} I_1^2(t, z), \quad (1b)$$

$$\frac{\partial N(t, z)}{\partial t} = \frac{\beta_{\text{TPA}}}{2h\nu_1} I_1^2(t, z) - \frac{N(t, z)}{\tau}. \quad (1c)$$

Equation (1a) describes the propagation of a weak probe field amplitude $A_2(t, z)$, where $\alpha_{l,2}$ is the linear transmission loss at the probe wavelength, σ_{FCA} is the FCA coefficient, $N(t, z)$ is the free-carrier density, β'_{TPA} is the non-degenerate TPA coefficient, and $I_1(t, z)$ is the intensity profile of the pump. The evolution of the pump is described by Eq. (1b) where $\alpha_{l,1}$ is the linear transmission loss at the pump wavelength and β_{TPA} is the degenerate TPA coefficient. In these equations we have assumed that the probe is so weak that it does not induce any nonlinear effects and that the value of σ_{FCA} is constant for the closely spaced wavelengths of the pump and probe. Finally, the time varying TPA-induced free-carrier density $N(t, z)$ is determined by the rate equation Eq. (1c) where h is Planck's constant, ν_1 is the pump frequency, and τ is the carrier lifetime. We solve this set of equations for two different scenarios as investigated experimentally in the following section. The first assumes a strong pump and weak probe, both of which are at $\lambda_1 \sim 1540\text{nm}$ so that $\beta'_{\text{TPA}} = \beta_{\text{TPA}}$, i.e., a degenerate TPA process with β_{TPA} the only free parameter. The second scenario involves a pump at $\lambda_1 \sim 1540\text{nm}$ and weak probe signal at $\lambda_2 \sim 1570\text{nm}$, where β'_{TPA} is now the free parameter.

3. Experiment and Characterization

The setup for the degenerate TPA experiment is illustrated in Fig. 1(a). A 650fs, 40MHz mode-locked fiber laser operating at 1540nm was split into a high power pump pulse ($\sim 250\text{W}$ coupled peak power) and a weak probe pulse ($\sim 10\text{mW}$ coupled peak power). The probe is modulated using an optical chopper so that a lock-in amplifier (LA) could be used to discriminate between the pump and probe signal. The delay line varies the temporal spacing between the probe and pump where an autocorrelator (AC) allows real-time view of the overlap between the two pulses. The a-Si:H core fiber used in these experiments was similar to that used in our previous nonlinear transmission measurements [12], with a core diameter of $5.6\mu\text{m}$, a length of 2cm and a linear loss of 1.7dB/cm at 1540nm. The pulses were coupled into, and out of the core using two 40x objective lenses with a numerical aperture of 0.65. The absorption of the probe as a function of delay is plotted in Fig. 1(b). This curve clearly shows the ultrafast response due to TPA, following which a rapid recovery occurs due to carrier relaxation (on the order of hundreds of femtoseconds) before slower recombination mechanisms take place [2,3]. This slow recovery due to FCA results in the depressed floor relative to the negative delay times and from this we can estimate a free carrier density of $N \sim 0.6 \times 10^{21} \text{m}^{-3}$ [14]. Solving Eqs. (1a)–(1c) with $\sigma_{\text{FCA}} = 1 \times 10^{-16} \text{cm}^2$ [12] and $\tau \sim 100\text{ns}$ [15] we obtain a good fit for $\beta_{\text{TPA}} \sim 0.8 \text{cm/GW}$, as shown by the solid line in Fig. 1(b). This value of the TPA parameter is in

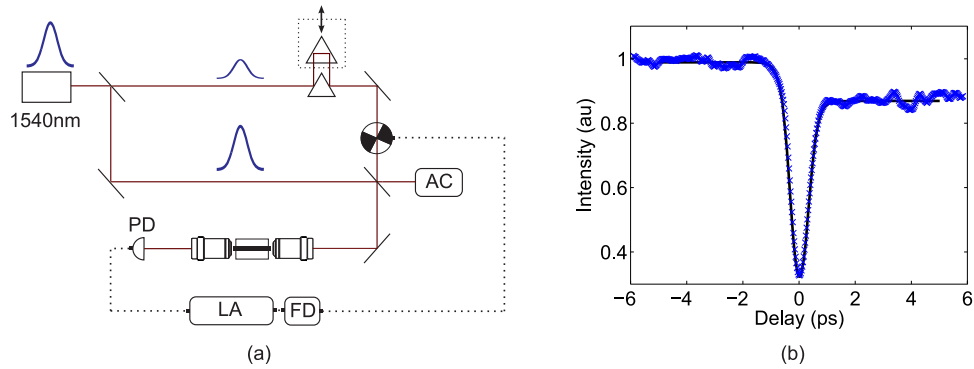


Fig. 1. (a) Degenerate TPA experiment. AC Autocorrelator, PD Photodiode, LA Lock-in amplifier, FD Frequency driver. (b) Measured degenerate absorption (blue crosses) together with the simulated fit (black line).

excellent agreement with our previous estimates using nonlinear absorption measurements [12] and with those reported for a-Si:H waveguides on-chip [1, 16]. The subpicosecond absorption within the probe pulse has a width of ~ 800 fs, which is only slightly broader than the original 650 fs pump, and exhibits an extinction ratio of ~ 4.5 dB.

To investigate non-degenerate TPA, the experimental setup was modified to generate a weak probe at a wavelength shifted from the pump as shown in Fig. 2(a). Here the pulses that propagate through the highly nonlinear fiber (HNLF) experience strong spectral broadening and the output is filtered by a bandwidth variable tunable filter (BVF) to select the desired wavelength. A minimum probe pulse width of 1 ps is achieved by maximizing the bandwidth of the filter centered at 1570 nm. After propagation through the a-Si:H fiber the pump and probe were separated using a blazed diffraction grating and a pinhole was positioned to isolate the 1570 nm probe. The non-degenerate absorption curves are plotted in Fig. 2(b) for three different pump powers, as labeled in the legend. We obtain a good fit for all the selected powers with $\beta'_{\text{TPA}} \sim 0.49$ cm/GW at 1570 nm. This estimated value is slightly lower than that obtained for the degenerate TPA parameter due to the lower photon energy of the probe, as predicted by the two-parabolic band model [17]. Again, from the levels of the depressed floors we can estimate

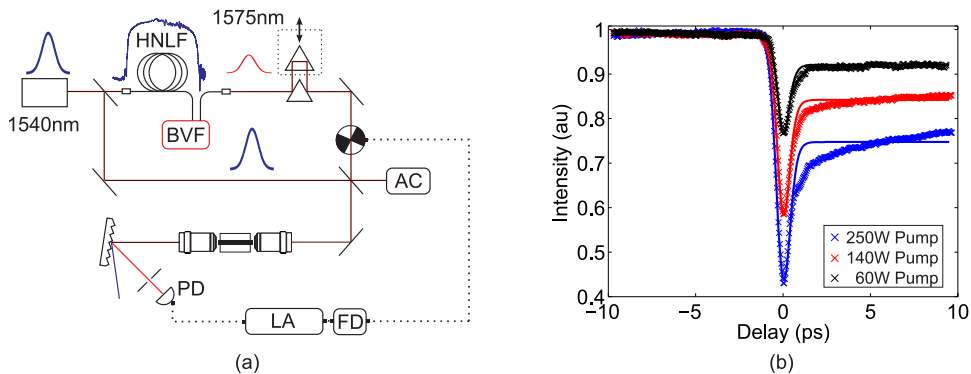


Fig. 2. (a) Non-degenerate TPA experiment. HNLF Highly nonlinear fiber, BVF Bandwidth variable tunable filter. (b) Measured non-degenerate absorption (crosses) as a function of pump power together with the simulated fits (solid lines).

the carrier densities as $N \sim 1.1 \times 10^{21} \text{ m}^{-3}$, $0.7 \times 10^{21} \text{ m}^{-3}$, and $0.4 \times 10^{21} \text{ m}^{-3}$, for the highest to lowest pump powers, respectively. Compared to the degenerate experiment, there is almost twice the number of carriers generated in the non-degenerate case for the 250 W pump, whilst a similar number are generated for the lower pump powers. We also note that for the higher pump powers, an elongated carrier relaxation feature can be seen that is not reproduced by the simulations. At this stage the precise cause of this elongation is not known, though it could be due in part to the difference in the pump-probe pulse widths and/or the generated carrier densities, and further investigations are currently ongoing. The modulated absorption width is estimated to be $\sim 1.1 \text{ ps}$, indicating only a minor temporal broadening relative to the incident probe pulse, and the measured extinction ratio for a pump peak power of 250 W is $\sim 3.5 \text{ dB}$. This observed reduction in the extinction ratio, relative to the degenerate experiment, can be primarily attributed to the lower value of the non-degenerate TPA parameter. Thus, as β'_{TPA} is predicted to increase for a decreasing probe wavelength [17], we expect that larger modulation depths could be obtained by simply using a shorter probe wavelength. By measuring the band edge of our a-Si:H material it should be possible to obtain an accurate estimate for the TPA cutoff, allowing for the extinction ratio to be optimized.

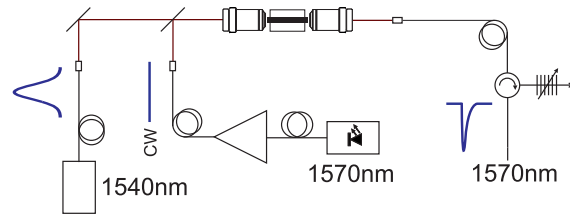


Fig. 3. Non-degenerate TPA experiment for a CW probe.

As a final experiment we demonstrate ultrafast XAM of a weak CW signal via non-degenerate TPA as illustrated in Fig. 3. Here the probe source is a laser diode operating at 1570nm and the coupled input power is $\sim 500 \mu\text{W}$. The impulse response of the pump and the filtered probe, as measured on a bandwidth-limited 30 GHz RF oscilloscope are shown in Fig. 4(a), where the modulated probe appears as an inverted imprint of the pump. Although, it is not possible to characterize this low power dark pulse using nonlinear pulse measurement techniques such as autocorrelation and frequency-resolved optical gating (FROG), following our pump-probe measurements we can estimate the response time to be on the order of the 650 fs pump width. Again it is clear from the depressed floor following the modulation that there is a slow recovery due to FCA. Expanding the time scale in Fig. 4(b) it is evident that the material recovery is on a similar time scale to the repetition rate of the pump, which will ultimately limit the operation speed. An exponential fit to the decay curve reveals a lifetime of $\sim 87 \text{ ns}$, as expected for a micron sized silicon core. For high bit rate applications, this lifetime could be reduced by using smaller core fibers, which have a larger surface defect density, and values as low as $\tau \sim 400 \text{ ps}$ have been measured in a nanoscale waveguide with a a-Si:H core [3]. Importantly, previous experiments in nanoscale waveguides have shown that it is possible to reduce the lifetime to a level that minimizes the extent of the lowered floor following the modulation so that the operation speed is no longer limited by FCA [11]. In addition, the tighter mode confinement offered by the smaller core sizes will also allow for the pump powers to be reduced to levels more commonly employed in telecommunication networks.

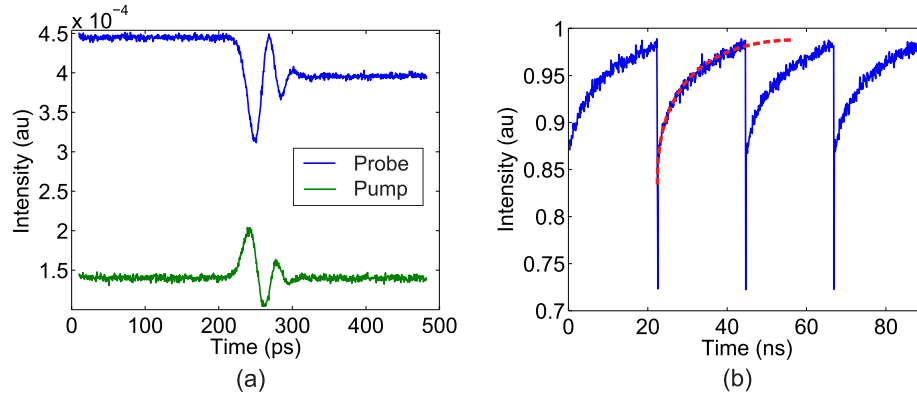


Fig. 4. (a) Impulse response of pump pulse and modulated probe. (b) Carrier relaxation where the fitted (red) curve reveals $\tau \sim 87$ ns.

4. Conclusion

We have characterized the degenerate and non-degenerate TPA parameters in a hydrogenated amorphous silicon core fiber using pump-probe experiments. The results obtained are in good agreement with previous reports for silicon waveguides on-chip and demonstrate the potential for these fibers to find use in ultrafast modulation or switching schemes [13]. XAM of a weak CW probe has indicated that the modulation rate is currently limited by the relatively long carrier lifetime in the micron sized core. By reducing the core size, these fibers should be capable of operating at the high bit rates necessary for telecommunications applications.

Acknowledgments

The authors acknowledge EPSRC (EP/G051755/1 and EP/G028273/1), NSF (DMR-0806860) and the Penn State Materials Research Science and Engineering Center (NSF DMR-0820404) for financial support. A. C. Peacock holds a Royal Academy of Engineering fellowship.